Advances in Science and Technology Research Journal

Advances in Science and Technology Research Journal 2021, 15(1), 230–244
https://doi.org/10.12913/22998624/132279
ISSN 2299-8624, License CC-BY 4.0

Received: 2020.12.10
Accepted: 2021.01.21
Published: 2021.02.01

Experimental Verification of Standard Recommendations for Estimating the Load-carrying Capacity of Undercut Anchors in Rock Material

Józef Jonak[1*], Robert Karpiński[1], Michał Siegmund[2], Anna Machrowska[1], Dariusz Prostański[2]

[1] Department of Machine Design and Mechatronics, Faculty of Mechanical Engineering, Lublin University of Technology, Nadbystrzycka 36, 20-618 Lublin, Poland

[2] KOMAG Institute of Mining Technology, Pszczyńska 37, 44-100 Gliwice, Poland

[*] Corresponding author's email: j.jonak@pollub.pl

ABSTRACT

The recommendations put forward in the International Standards for anchorage in concrete concerning the assessment of the load-carrying capacity of anchors (the pull-out force) embedded in natural rock material were verified. Regarding the predicted extent of surface failure we have shown, in earlier studies, substantial discrepancies between the strength test results for anchorages in the rock mass and the established standard recommendations for anchorages in concrete. As regards the industrial practice and the goals of the reported project, simplified calculation procedures that will facilitate the selection of optimal configurations for the layout of anchor holes, while being computationally effective and applicable under the industry-specific conditions are sought.

Keywords: rock destruction, concrete breakout failure, empirical model, fracture mechanics, numerical modelling of fracture, rock mechanics.

INTRODUCTION

The issue of the load-carrying capacity of anchors is critical for any of its wide range of applications, which include fixing components and structural elements in concrete engineering structures. Given the cardinal importance of safety considerations in nuclear power plants or other strategic facilities, especially those located in the earthquake zone, there has been a further surge of interest in anchorage strength testing.

The objectives of this research are to determine whether anchorage in rock can be utilised as a rock fracturing technique under exceptional mining conditions. The undercut anchors are embedded and subsequently pulled out together with the breakout prism that forms around the fastener. The method could replace the standard mining methods, such as explosives or mechanised mining systems, under the conditions that exclude their application, e.g. during the rescue operations in collapsed extraction galleries, under volatile conditions of high methane concentrations or in modernisation of engineering facilities.

Concrete is regarded as a global composite with a homogeneous internal structure. However, its specific strength will depend on the size of aggregate grains, the rock material from which the grains are obtained and their proportion to the cement content. This also translates into the load-bearing capacity of the anchors fixed in concrete or, generally speaking, into the size of the breaking force of the anchor [1].

The properties of rock materials are thereby largely dependent on the mineral from which the grains are derived, the size of the mineral grains and the type of binder. However, there is a strong dependence of e.g. the compressive strength on the stratification, the degree of fracturing or the rock sedimentation in the rock mass. The same

types of rocks, e.g. sandstones, may differ significantly in terms of strength. All these factors are the contributors to the anchor pull-out force or its load capacity (permissible with the assumed safety factor of its operating load).

The main challenge, which has been already confirmed in our preliminary research, is that due to the highly heterogeneous properties of rock material, both in terms of the internal structure and geometry, a number of existing standardised measures and methods become non-applicable [2]. In the study [3] and [4] it was shown that the parameters of the failure cone for concrete and rocks differ from each other. For rocks, the value of the angle of the cone failure is approximately 25°. In the experimental studies carried out under the conditions of Polish stone mines, the obtained values of this angle were by almost 40% lower. In study [5] it was found that the power exponents in empirical models of the dependence of the load capacity of the anchor in the function of anchoring depth are of the order of 1.6 and are slightly higher than for concrete. In research [6] it was found that the interaction of failure cones under the action of an anchor set in rocks has a much greater range than in concrete. The shape of failure surface and concrete breakout capacity of anchors predicted by the mechanism analysis are significantly affected by the ratio between the effective tensile and compressive strengths of concrete [7]. Experimental and analytical works are, thus, necessary to determine the actual range of the pull-out forces and volumes of breakout prisms occurring under particular sets of conditions in single- and multiple-anchor anchorage systems pull-out. As for the volume of the failure cone, there are several factors to consider, including the layout of anchors in the multiple-fastener systems and the energy consumption of the process. At present, breakout prism formation is reduced to a set of simplifying assumptions, particularly Cone Capacity Design (CCD), which are quite extensive and hence may not correspond with the natural rock material. The model of the cone failure mechanism as a result of anchor pull-out, which was developed in the 1960s, is overly simplistic and assumed that the breakout prism angle is equal to 45° [8, 9]. Although the failure was initially considered to occur on the cylinder side surface, it was later replaced by a cone. In the established models, an important role is assigned to the values of tensile stresses that arise as a result of the anchor pull-out. After scaling, they are determined from the compressive strength of the tested material and allow us to compute the load-carrying capacity of an anchor for a given effective embedment depth (h_{ef}).

At present, the most widely used method is the CCD-Concrete Capacity Design method, which is applied in the calculations of the load-carrying capacity of anchors; it assumes that the angle of the failure surface is 35° [10÷13], (Fig. 1.). This model assumes a cone angle of 35° with respect to concrete surface and constant tensile stress f_{ct} acting on the projected cone surface in uncracked concrete unaffected by edge influences or overlapping cones of neighbouring anchors. Under tension loading, the concrete capacity of a single anchor is calculated assuming an inclination between the failure surface and surface of the concrete member of about 35°.

For practical application, given the difficulty of determining the tensile strength of concrete (f_t), the CCD model introduces the conversion equivalent stress f_{ct} which is the projection of stresses f_t on the surface of the cone base, determined from the relationship:

$$f_{ct} = 0.3 f_{cc}^{0.5} \; N/mm^2 \qquad (1)$$

f_{cc} – Concrete compressive strength measured on cubes [MPa]

This undercut anchor is placed in a prepared hole at a required depth. The depth of the hole is correlated with the design of the anchor head and the planned effective embedment depth h_{ef}. The specific data is obtained from the manufacturer

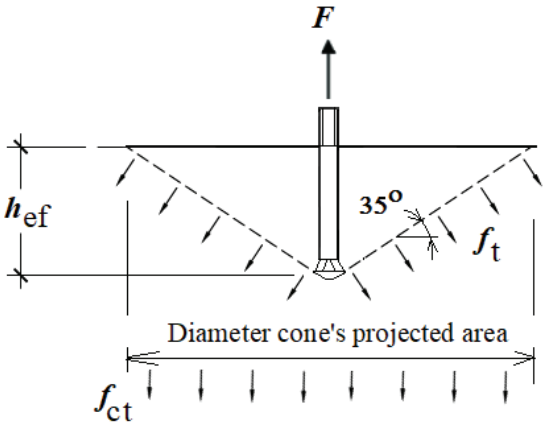

Fig. 1. CCD model of destruction in pull-out test: F – pulling force of the anchor, h_{ef} – effective embedment depth, f_t – tensile stress at the side of the cone equal to the tensile strength of the medium, f_{ct} – equivalent stress, being the projection of the stress f_t on the surface of the cone base

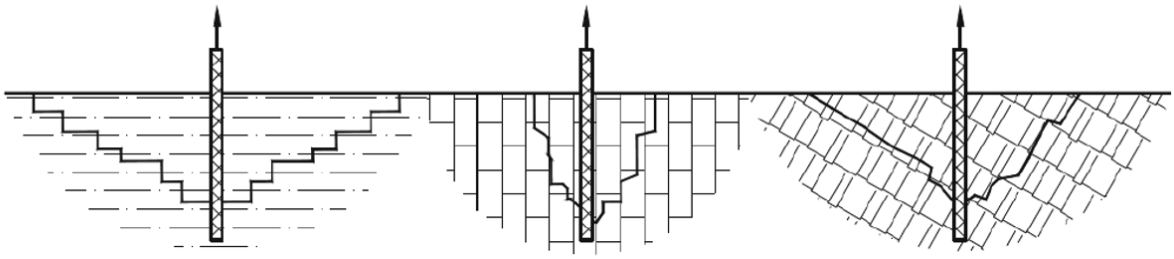

Fig. 2. Impact of rock structure on the extent of the destruction cone

catalogues. This value also influences the load-carrying capacity of the anchor or the failure force. Next, the torque and axial force from the impact applied using a hammer drill and a special device, act on the expansion sleeve. Such a load on the anchor sleeve causes it to expand at its conical end while undercutting the lower hole. When the anchor is loaded with an axial force directed to the bottom of the hole, the force begins to act on the walls of the undercut, having exceeded the critical value, causes a crack to form and propagate.

The presented model of destruction is adequate assuming that the concrete is a macro-scale, homogeneous centre. However, in the case of rock material, such an assumption is a considerable simplification. The potential stratification of the medium may play a critical role as it can affect to a greater or lesser extent the propagation and size of the failure surface and change the potential load capacity of the anchor or the force required to remove it. For deep embedments, this aspect was signalled by Wyllie [14], as shown in Figure 2. Extensive numerical research on this issue was conducted by e.g. Panton [15].

In the case of undercut anchors, however, there is a distinct paucity of experimental and theoretical evidence in the field, which additionally justifies conducting work in the presented subject matter.

Existing methods for estimating the load capacity of mechanically fixed anchors – state of the art

Considering the effect of the anchor on the material, the selection of the right model (e.g. elastic or plastic) may be a decisive interfering factor in various calculations. An example would be the analysis carried out by Brincker et al. [16], where certain simplified assumptions were made regarding the stress distribution in the failure cone that was established from a model based on the theory of elasticity and plasticity. From the analyses, it emerged that the assumption of stress distribution derived from the theory of plasticity produces estimations in the upper-range, while the linear-elastic model gives results in the lower range of the fracture stress and, consequently, the anchor pull-out force. The tensile stress estimates based on the theory of plasticity produced the results of up to 2.5 times higher than the values calculated from the theory of elasticity.

Other researchers, Eligehausen & Sawade [17] or Ljungberg [18], based their considerations on ELFM and proposed an analytical/theoretical model in which the anchor load-carrying capacity (resistance to pull-out) F_{EGF} [N] is a function of the a_1 factor, embedment depth h_{ef} [mm], modulus of elasticity of concrete E and concrete fracture energy G_F. The critical value of this coefficient, a_1 = 2.1(N$^{0.5}$/mm$^{0.5}$), links the anchor load-carrying capacity (maximum load) with the length of the already propagating crack compared to the extrapolated total crack length to the concrete surface. This analysis also shows that the maximum value of the anchor pull-out force occurs for approximately (0.43–0.45) L_c (length of cone side surface). The cracking propagates (producing failure surface) at an angle of 37.5° to the free surface of the base material. The tensile strength of concrete is, therefore, exceeded long before the anchor is removed.

A number of analytical models describing the impact of various anchorages in base materials are currently in use. In their works [19, 20], Asmus et al. presented the effect of the anchor head design on the load-carrying capacity. Ballarini et al. [21, 22] described the models of crack growth based on linear-elastic fracture mechanics, while Carpinteri [23] compared the effectiveness of modelling using linear and nonlinear fracture mechanics. In a different work, Karihallo [24] studied the impact of concentrated force and continuous load in a "penny crack" on the crack

path. Another study [25] presented a model for load distribution in a cone head for a simplified estimation of the load-carrying capacity of anchorages. Several analytical models of the effect of anchors on concrete have been presented. The study [26] showed that the concrete resistance to the anchor pull-out force can be attributed to the area within the surface with a radius of 1.7 times the embedment depth. They exhibited a varying degree of simplification, which enabled the analysis of the anchor loading progression, the mechanism of concrete failure under peak loads or the extent of failure surface during the formation of the breakout prism. In [27] it was shown that the operational reliability and load-bearing capacity of torque-controlled expansion bolts depends on the internal and external friction of the anchor. The shape of failure surface and concrete breakout capacity of anchors predicted by the mechanism analysis are significantly affected by the ratio between effective tensile and compressive strengths of concrete [7]. The article [28] investigated the crack growth mechanism and the concrete fatigue strength during an anchor bolt pullout test under fatigue load.

Brincker et al. [16] proposed a simplified mechanical model of concrete failure, rooted in the assumptions of linear fracture mechanics, for the estimation of the anchor load capacity, breakout prism dimensions and angle depending on the effective embedment depth and the brittleness number of the base material. The model assumes that the type of problem is planar, the failure cone and the surrounding material perfectly rigid and the layer representing the gap is elastic. In addition, the crack path is assumed to be linear and the angle is φ. Finally, the deformation is a result of the movement of the rigid body, i.e. from the rotation around the point where the crack path comes into contact with the (concrete) material surface.

In Zhao's simplified cone [29], 2 stress zones were distinguished and separated by the ~$0.5h_{ef}$ point. The pull-out force was derived from:

$$N_{ue} = 15 f_{cc}^{0.5} h_{ef}^{1.5} \tag{2}$$

where: f_{cc} – cube compressive strength of concrete, h_{ef} – effective embedment depth.

In the Yang and Ashour model [7], the material is a perfectly plastic material, as per modified Coulomb failure criteria. A simplified, two-linear model (2D), which was also proposed, assumes the failure surface in the form of two conical failure surfaces with the breakout angle α for greater depths of failure and α for smaller ones. In the event of damage to material continuity, the breakout concrete elements can be considered as two separate rigid blocks in relative motion.

The models presented in the works of Vogel & Ballarini 1999 [30] and Piccinin [31] served to analyse the crack path propagation depending on the base material parameters, stresses in the crack region as well as the technological and design parameters of anchoring. The general mathematical relationship for determining a load-carrying capacity of an anchor is given by:

$$\mathrm{P_{u,LEFM}} = \max\left[\mathrm{f_1}\left(\frac{\mathrm{l}}{\mathrm{d}}, \frac{\mathrm{d}}{\mathrm{c}}, \vartheta\right)\mathrm{K_{Ic}d^{1.5}} + \mathrm{f_2}\left(\frac{\mathrm{l}}{\mathrm{d}}, \frac{\mathrm{d}}{\mathrm{c}}, \vartheta\right)\sigma\right] \tag{3}$$

where: c, d, l – anchor head diameter, effective embedment depth and crack length, ϑ – Poisson's ratio, σ – normal stress, K_{Ic} – critical stress intensity factor for mode *I*.

Rui S. Camposinhos [32] developed the semi-empirical model (semi-empirical formulations)

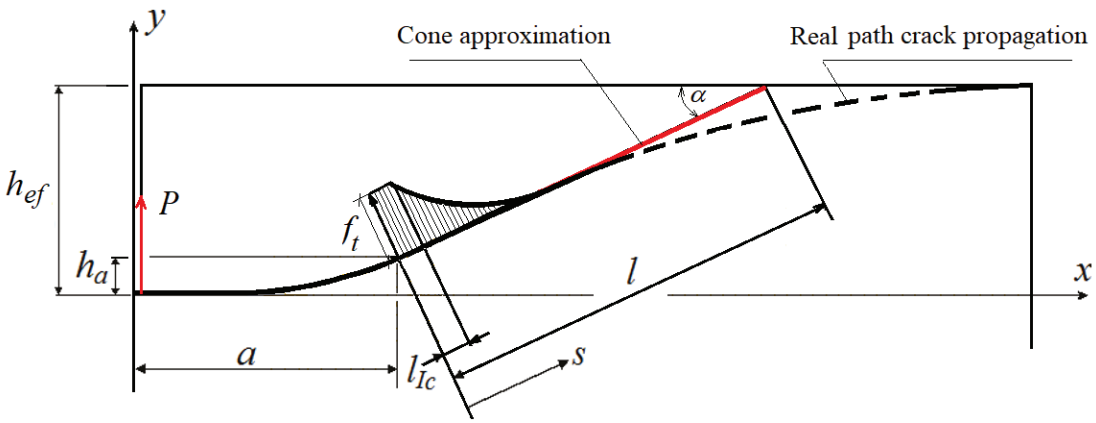

Fig. 3. A mechanical model of crack propagation in anchor pull-out: l – simplified crack path length, h_{ef} – effective embedment depth, f_t – tensile strength, α – angle of failure cone, l_{Ic} – cohesive zone length P – force applied to anchor, a, h_a – coordinates of the crack tip

based on classical strength calculations accounting for the notch effect, which causes stress concentration at a specific place in the structure. A serious limitation of the model consists in that it requires experimental calibration (determination of stress concentration factors) for each type of rock.

A model proposed in one of our former studies [2] describes real crack propagation under anchor pull-out (Fig. 3).

The shape of the breakout prism was simplified to approximately conical, which is not consistent with the computer simulations; however, given that it only serves to determine the critical force, only the angle around which the maximum strength was recorded in the computer-aided simulations is significant. The predicted critical force occurs at the point where the crack path is approximately equal to the embedment depth ($a = \sim h_{ef}$).

The tensile stress distribution from crack tip to the hypothetical point of rock fracture, i.e. the "cohesive zone" was derived from the Barenblatt hypothesis [33], which permits accounting for microcracking preceding the discrete crack propagation. Along the cohesive zone length l_{Ic}, it is rectangular and with the intensity equal to tensile strength, while outside the stress zone it decreases to reach zero at the rock surface.

Numerous models reported in the literature are dedicated to analysing the effect of cyclic anchor loading, which may occur during earthquakes, on their load-carrying capacity (e.g. Zaidir et al. [28]).

The majority of the models presented in the preceding paragraphs require experimental determination of certain variables, such as the stress concentration factor for a specific group of rocks; otherwise, the calculations could not be considered reliable. For that reason the use of these fracture models in industrial practice would be rather counter-productive. The key reason is the difficulty with the experimental determination of stress intensity factor or fracture energy of the material that shows high scatter of results. Other models may necessitate further and complicated calibration to predict the values of the required factors. Experience shows [2] that for certain sandstones, the cracking energy is quite high, the material failure (cracking) occurs rapidly and the fractured pieces scatter uncontrollably around the testing stand. Under such conditions, determining such an important parameter as the cohesive zone length l_{IC}, becomes impossible, even when high-speed cameras are employed.

From the analysis of scientific literature, it emerges that the procedure for determining the load-carrying capacity of anchors that is most widely used nowadays is based on the following relationship [11]:

$$F_{CCD} = k_{nc} f_c^{0.5} h_{ef}^{1.5} \tag{4}$$

where: k_{nc} ($N^{0.5}/mm^{0.5}$) – calibration factor, accounting for the anchor type, condition of the base material, embedment depth, etc, F_{CCD} – the load-carrying capacity of an anchor, according to Concrete Capacity Design, (kN).

According to Fuchs et al. [11] and Eligehausen et al. [10], the cube and cylinder compressive strength of concrete are governed by the relationship $f_c \approx 0.85 f_{cc}$. Therefore, the cube compressive strength of concrete (f_{cc}) should be given in an equation instead of the cylinder compressive strength of concrete (f_c), then the calibration factor k_{nc} will be equal to 15.5 instead of 16.8 [34].

The results from the experimental tests show that the exponents for f_c, equal to 1.58-1.67 and 0.8766, differ significantly from the ones postulated in the CCD procedure (1.5); however, they correspond to the recommendations for the determination of the anchor pull-out force in concrete set out in the ACI-318 standard [35, 36] but for greater embedment depths. According to this standard:

$$F_C = k_{nc} f_c^{0.5} h_{ef}^{5/3} \Leftrightarrow F_C = k_{nc} f_c^{0.5} h_{ef}^{1.666} \tag{5}$$

where: $k_{nc} = 16$, but for 280 mm $\leq h_{ef} \leq$ 635 mm (11 in $\leq h_{ef} \leq$ 25 in).

The recommendations put forward in the International Standards for anchorage in concrete concerning the assessment of the load-carrying capacity of anchors (the pull-out force) embedded in the natural rock material were verified experimentally. Regarding the predicted extent of surface failure, we have shown in earlier studies the substantial discrepancies between the strength test results for anchorages in the rock mass and the established standard recommendations for anchorages in concrete. As regards the industrial practice and the goals of the reported project, simplified calculation procedures that will facilitate the selection of optimal configurations for the layout of anchor holes, while being computationally effective and applicable in the industry-specific conditions are sought. In situ tests were carried out within the framework of a series of projects. These tests improve the knowledge on the process of rock destruction under load from undercut anchors.

MATERIALS AND METHODS

A number of tests were carried out on undercut anchors fixed in rock material taken from sandstone seams (2 extraction plants) or directly fixed in the natural rock mass (1 underground mine – sandstone seams, 1 sandstone extraction plant).

The loosening of rock specimens from a solid rock was carried out for four different types of rocks at four mines in order to obtain the material of diverse strength properties:

An attempt was made to fix the anchors in the drilled holes as parallel as possible to the predicted layering. Perpendicular stratification resulted in a considerable size of rock material destruction.

A characteristic feature of the tests was an extensive variation in the condition and structure of the rocks or their compressive strength, which depended on the mining plant where the tests were conducted. In addition, the rocks either showed considerable stratification (Brenna) or uniform and compact structure (Zalas). In Guido mine, the rocks in the walls of the testing gallery were compact, dry and subjected to vertical pressure of the rock material of unknown characteristics. Otherwise, the tests were conducted on extracted blocks or exposed sandstone bed.

In the laboratories of the Department of Geomechanics and Underground Construction of the Faculty of Mining and Geology of the Silesian University of Technology, the specimens were subjected to the strength tests. The tests were in full compliance with the recommendations of the International Society of Rock Mechanics (ISRM) in terms of the accuracy of sampling, instruments and testing methodology.

Cylindrical samples, d = 42 mm, and various slenderness factors h/d were prepared for testing. The Axial compression tests and tensile tests were carried out using the Brazilian method.

In the compression tests, measurement consistency c and internal friction angle φ were determined for the rocks studied. The shear force in the compression test was measured at fixed shear angles of 15° and 30° in order to determine the maximum normal stress σ_{nmax} and tangential stress τ_{tmax}.

Table 1 shows the mechanical characteristics of rocks in individual mines.

Experimental tests

The undercut anchor testing was carried out in 4 stone mines (Braciszów, Brenna, Guido, Zalas) [5]. The mobile test set-up was composed of: a jig frame for the testing actuator device with three height-adjustable supports, a hydraulic cylinder, a hand pump set with a pressure gauge and a digital recorder.

This type of anchor is placed in a prepared hole at a required depth. Then, the torque and axial force from the impact applied using an impact drill and a special device act on the expansion sleeve. Such a load on the anchor sleeve causes it to expand at the conical end of the anchor while cutting a hole at the bottom. After the anchor is loaded with an axial force generated by a hydraulic actuator, the force starts to act on the undercut walls, which, when exceeded, causes a crack to form and spread, leading to the rock element being detached.

The specific focus of tests was selected relative to the mechanical parameters of rocks in particular mines, e.g. the effect of the anchor embedment depth on the behaviour of the pull-out force, the size of the failure cone or the dimensions of the undercut.

As a result of the tests carried out within the project, 115 successful solid rock loosening trials were performed using a fixed undercut anchor.

The influence of the rock layering becomes apparent in the presented time courses of the anchor pull-out force, which exhibit notable oscillations.

Table 1. Mechanical parameters of the studied rocks

Mine	f_c (MPa)	Standard deviation	f_t(MPa)	Standard deviation	$k = f_c/f_t$	φ (^{0})	c (MPa)	Rock	Description
Zalas	106.5	23.86	5.9	1.91	18.1	54	8.6	porphyry	Deck strongly undulating
Braciszów	155.3	29.17	8	0.64	19.41	49.5	14.5	sandstone	Sandstone strong, compact
Brenna	58.8	9.29	3.9	1.17	15.1	53	6	sandstone	Sandstone layered, weak
Guido	97.4	25.52	6.2	0.94	15.7	49.6	11.9	sandstone	Sandstone compact, medium strength

f_c – compressive strength, f_t – tensile strength, c – cohesion, φ – angle of internal friction, k – strength asymmetry factor

Clearly, the destruction of randomly distributed rock layers is the primary cause of the observed oscillations in the force. In case of failure in the structure of the compact and very strong porphyry from the "Zalas" mine, the force transmissions are minimal. Once the critical value of the force destroying the structure is reached, the failure with the pull-out of the "pseudo-cone" proceeds rapidly.

RESULTS AND DISCUSSION

The shape and dimensions of the failure surface are shown to be strongly correlated with the rock formation on which the experiment was conducted. Medium-strength solid sandstones tend to break out as symmetrical forms similar to those obtained in concrete, but are more flattened towards the end. As a result, the crack propagates over a longer distance from the anchor axis as measured on the free surface of the rock. Consequently, the volume of the cone is considerably higher than in concrete. The shape (form) of the failure cone is accurately represented by a cloud of points obtained from a 3D scan of the breakout prism. Its cross-sections were used for the comparison of the failure surface obtained from 2D and 3D numerical simulations of the cone failure in the undercut anchor pull-out tests (this subject, however, is discussed in other published works that were based on the conducted in-situ tests). The failure surfaces observed in

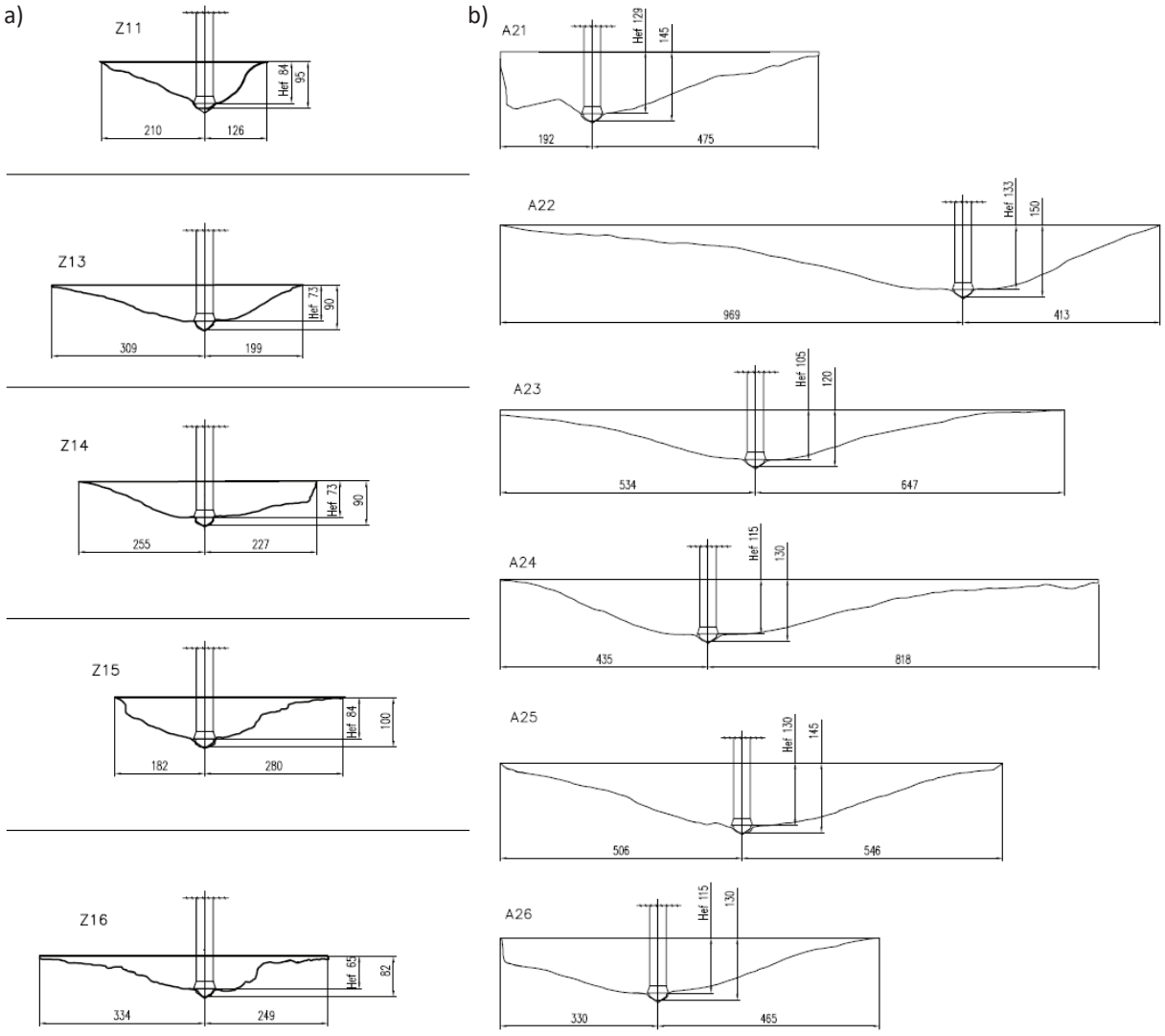

Fig. 4. Outline of the failure surface in the axial section of the "destruction cone": a) "Zalas" mining and b) "Brenna" mining. Letters A and Z denote the mines and the digits – the number of the measurement (the system used for documentation purposes)

the compact sandstone exhibit substantial differences (in the axial cross-section through the anchor) from those observed in concrete and other rocks: their outline is clearly paraboloidal. The obtained cones display high resemblance to the conical failure mode in the concrete reported by Ballarini et al. [36], which was, however, produced with the use of shorter anchors embedded in a brittle material. The difference in the design was more favourable compared to the undercut anchors considering tensile stress generation in the rock, which may be the key factor determining the observed shape of the propagating crack. The bedding of the porphyry is clearly visible, with its layers diagonal to the anchor axis. The high-degree roughness is indicative of the abrupt formation of the failure surface, as it traverses the individual "segments" of the rock.

The shape (form) of the failure cone is transformed into a cloud of points using the 3D laser scanning obtained in the breakout test. The digital data processing produces a highly accurate representation of the breakout prism. The cross-section of the failure cone failure (or an approximated outline of the breakout prism obtained in the anchor tensile test) is shown in Fig. 4a and Fig. 4b.

For homogeneous materials, typical of the pull-out test, the actual cross-section of the failure surface is illustrated by the cross-section A25 column 'b' in Figure 4. This is an axially symmetrical form. Any disturbance of the structure, discontinuity and cracking of the material is manifested by an irregular course of crack propagation, a rapid change of its propagation direction and a rapid exit to the free surface. This is perfectly illustrated by the cross-sections of the surface of the damage shown in Figure 4.

For the rock structures studied, typical relationships of the pull-out force as a function of embedment depth are shown in Figure 5.

The chart in Figure 5 indicates that the relationships are largely exponential (as it is in the case of concrete), given that the power exponent value was higher than one (1.58–1.67). However, the relationship observed in the Braciszów mine (0.8766) is an exception here. All results obtained from the tests, including extreme values, have been included in the analysis. As each measurement was supplied with an appropriate metric – describing in detail the crack propagation in a given rock structure including any artefacts discovered in

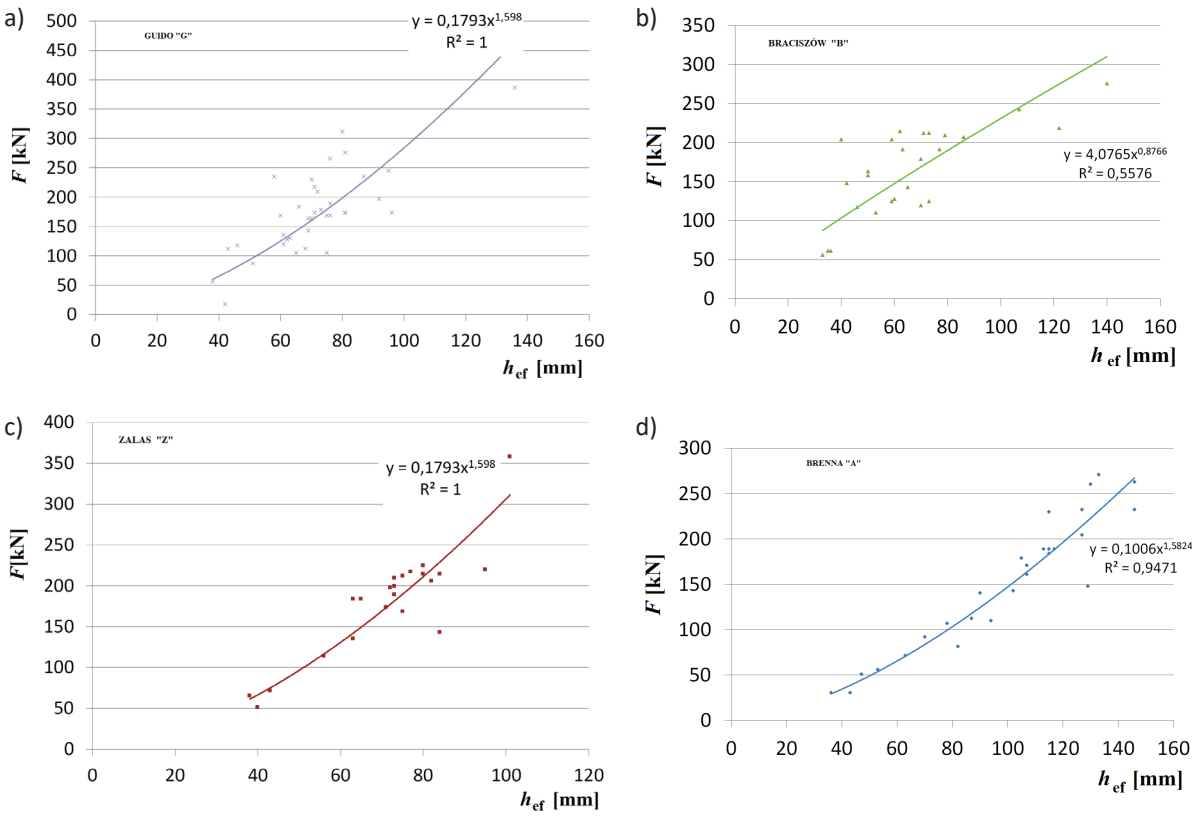

Fig. 5. Pull-out force F in relation to effective embedment depth h_{ef} for different mining (rock types): a) Guido, b) Braciszów, c) Zalas, d) Brenna

the structure, e.g. hidden cracks or local changes in stratification, to improve the understanding of the failure mechanism – these results were also included in the statistical analysis. As a result, the correlation coefficients may appear rather low; nevertheless, their inclusion was important from the perspective of further investigations into the relationships between the value of the pull-out force and the crack propagation in the medium as well as the role of the condition of specific deposits and the rock structure described in Table 1.

The tested rock specimens had been extracted from different locations and displayed diversified internal structure, as specified in Table 1. The material was characterised by a relatively high tension-compression asymmetry (f_c/f_t ratio). Sedimentary rocks (typically occurring in Brenna mine) displayed evident bedding, i.e. their individual layers were separated by parallel thrust planes. These planes are responsible for the lowest rock strength. In Brenna mine, however, the rock was characterised by relatively high homogeneity, especially on the macro scale – corresponding to the maximum embedment depths. In the case of Zalas mine, apart from the stratification planes, other planes that also contributed to decreasing the rock strength were detected. These layers were formed at a later stage as a result of orogenic, that is tectonic forces, and are particularly susceptible to cleavage – i.e. tectonic foliation manifesting itself predominantly in highly folded rocks. It is due to these factors that the rock strength parameters determined in the experiments display high-degree divergence, particularly with respect to the compressive strength (fc) and tensile strength (ft). Regarding fc, the highest standard deviation was recorded in Braciszów (29.17) and Zalas (23.86) mines. As a result, considerable discrepancies between the results from anchor tensile tests were observed between particular mines (Fig. 5).

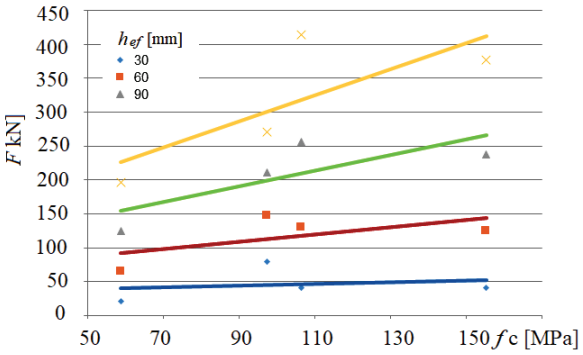

Fig. 6. Pull-out force F in relation to compressive strength f_c and for to effective embedment depth h_{ef}

As shown in Figure 5, the largest scatter of results was observed in the Guido and Braciszów mines. In the former, the discrepancies may not have been caused by the rock structure alone, which was relatively homogeneous, but rather by the stress concentration in the mining wall where the tests were conducted. In underground mines, the pressure of the rock mass is relative to the depth at which the extraction is carried out and the distance from the free surface. In this case, for each embedment depth, a different value of stress along the axis of the anchor should be expected, which may ultimately affect the final results of the measurements (also inducing local microcracking during anchor pull-out). In Brenna mine, the measurements were carried out in the layers of homogeneous sandstone of considerable thickness (in relation to the anchoring depth). The failure surfaces can be treated here as exemplary and are the closest in nature to those typically obtained in concrete (which on the large scale is treated as a homogeneous medium).

Figure 6 shows the linear relationship between the pull-out force as a function of the compressive strength of rock f_c and the effective embedment depth h_{ef}.

Table 2. Approximation relationships of the actual results of the anchor pull-out force as a function of the strength of the tested rocks f_c and the effective embedment depth h_{ef}

Mining	Rock	Approximating function	In situ value of force F (kN), h_{ef} = 100 mm
Brenna	Sandstone layered, weak	$F = 0.1006 h_{ef}^{1.5824}$	147.03
Zalas	Porphyry, strongly corrugated layers	$F = 0.1431 h_{ef}^{1.598}$	296.96
Guido	Sandstone compact, medium strength	$F = 0.1793 h_{ef}^{1.6652}$	306.22
Braciszów	Sandstone strong, compact	$F = 4.0765 h_{ef}^{0.8776}$	232

Table 2 summarises the obtained approximation dependencies of the results from in situ tests for individual mines, which are also presented in Figure 5, in the description of the curves approximating individual measurement results. In order to make comparisons possible, for the assumed equal anchoring depth h_{ef} = 100 mm, the pulling forces of the anchor *F* embedded in the given rock type were determined.

The relatively large spread of results in Figure 6 is mainly due to the heterogeneity of the internal structure of the studied rock materials.

The obtained values constituted reference for the values determined from the dependencies used in current standards and recommendations, but concerning concrete, as discussed in Section 1. In the first phase of the analysis, according to the functional dependencies given for concrete, using the assumed embedment depth, the compressive strength of the tested rocks and recommended values of calibration coefficients, the potential values of anchor load capacity in the tested rocks were determined. The values determined using this procedure are much lower than those obtained in the field tests. The results obtained for each type of rock, each with different compressive strength and structure described earlier, are presented in Tables 3-6.

In order to enable the use of empirical formulas adequate for concrete to estimate the load capacity of anchorage in rock material of a highly homogeneous internal structure, for each rock studied, the calibration coefficients in the calculation procedures in use so far were verified. The results are presented in Tables 3-6, for each rock case separately.

Considering the heterogeneity and variation in the internal structure of the rocks, the tables below present the values obtained from the existing recommendations for concrete, with a view to provide a broader understanding of how the anchor pull-out force behaves under different rock strength conditions. An attempt was also made to determine the changes in potential calibration factors (k_r), which correlate the results from the in-situ tests and existing functional relationships, using the formula below:

$$k_r = \frac{F}{\frac{N_u}{k_{nc}}} = \frac{k_{nc}F}{N_u} \tag{6}$$

where: N_u – force determined from a given formula (point 1.1), k_{nc} – calibration factor in a given formula F – force determined experimentally.

We are convinced that, among others, the main factor which heavily contributed to the scatter of results reported in this section is the considerable diversity of mining and geological conditions concerning the sandstone beds at testing sites.

Table 3. Brenna mine, h_{ef} = 100 mm

Eq. No.	Remark	Formula	N_u [kN] according formula	Ratio N_u/F	Ratio $k_r = \frac{k_{nc}F}{N_u}$
1	45 – degree cone model (37)	$N_u = 0.3 f_c^{0.5} \pi h_{ef}^2 \left(1 + \frac{d_h}{h_{ef}}\right)$	104.07	0.71	0.42
2	LEFM Eligehausen and Sawade (16)	$N_u = 2.1\left(E_c G_f\right)^{0.5} h_{ef}^{1.5}$	140.94	0.96	2.19
3	CCD method (10)	$N_u = 13.5 f_c^{0.5} h_{ef}^{1.5}$	103.52	0.7	19.17
	(12)	$15.5 f_c^{0.5} h_{ef}^{1.5}$	118.86	0.81	19.17
	(36)	$17 f_c^{0.5} h_{ef}^{1.5}$	130.36	0.89	19.17
4	CCD method (35,38) h_{ef} ≤ 280 mm	$N_u = 6.585 f_c^{0.5} h_{ef}^{1.6667}$	108.56	0.74	8.19
		$N_u = 16.8 f_c^{0.5} h_{ef}^{1.6667}$	276.96	1.88	8.92
		$15.5 f_c^{0.5} h_{ef}^{1.6667}$	256.11	1.74	8.90

f_c – concrete cylinder compressive strength (N/mm^2), h_{ef} – effective embedment depth (mm), d_h – diameter of anchor head (mm), N_u – mean breakout capacity in uncracked concrete according to formula (N), F – mean breakout capacity in uncracked concrete according to on-site test (N), E_c – elastic modulus of rock, G_f – rock fracture energy

The current state of knowledge (e.g. [39]), including the co-author's own research (e.g. [40]), shows that in the case of layered materials, their strength parameters strongly depend on the direction of the applied load. The maximum compression strength occurs in

Table 4. Zalas mine, h_{ef} = 100 mm

Eq. No.	Remark	Formula	N_u [kN] according formula	Ratio N_u/F	Ratio $k_r = \frac{k_{nc}F}{N_u}$
1	45 – degree cone model (37)	$N_u = 0.3 f_c^{0.5} \pi h_{ef}^2 \left(1 + \frac{d_h}{h_{ef}}\right)$	140.06	0.47	0.63
2	LEFM Eligehausen and Sawade (16)	$N_u = 2.1\left(E_c G_f\right)^{0.5} h_{ef}^{1.5}$	-	-	-
3	CCD method (10)	$N_u = 13.5 f_c^{0.5} h_{ef}^{1.5}$	139.32	0.47	28.76
	(12)	$15.5 f_c^{0.5} h_{ef}^{1.5}$	154.80	0.52	29.73
	(36)	$17 f_c^{0.5} h_{ef}^{1.5}$	175.44	0.59	28.78
4	CCD method (35,38) $h_{ef} \leq 280$ mm	$N_u = 6.585 f_c^{0.5} h_{ef}^{1.6667}$	146.43	0.49	13.35
		$N_u = 16.8 f_c^{0.5} h_{ef}^{1.6667}$	373.58	1.27	13.35
		$15.5 f_c^{0.5} h_{ef}^{1.6667}$	344.4	1.16	13.36

f_c – concrete cylinder compressive strength (N/mm²), h_{ef} – effective embedment depth (mm), d_h – diameter of anchor head (mm), N_u – mean breakout capacity in uncracked concrete according to formula (N), F – mean breakout capacity in uncracked concrete according to on-site test (N), E_c – elastic modulus of rock, G_f – rock fracture energy

Table 5. Guido mine, h_{ef} = 100 mm

Eq. No.	Remark	Formula	N_u [kN] according formula	Ratio N_u/F	Ratio $k_r = \frac{k_{nc}F}{N_u}$
1	45 – degree cone model (37)	$N_u = 0.3 f_c^{0.5} \pi h_{ef}^2 \left(1 + \frac{d_h}{h_{ef}}\right)$	134.15	0.44	0.69
2	LEFM Eligehausen and Sawade (16)	$N_u = 2.1\left(E_c G_f\right)^{0.5} h_{ef}^{1.5}$	-	-	-
3	CCD method (10)	$N_u = 13.5 f_c^{0.5} h_{ef}^{1.5}$	133.23	0.44	31.03
	(12)	$15.5 f_c^{0.5} h_{ef}^{1.5}$	152.97	0.50	31.03
	(36)	$17 f_c^{0.5} h_{ef}^{1.5}$	167.74	0.55	31.04
4	CCD method (35,38) $h_{ef} \leq 280$ mm	$N_u = 6.585 f_c^{0.5} h_{ef}^{1.6667}$	140.04	0.46	14.40
		$N_u = 16.8 f_c^{0.5} h_{ef}^{1.6667}$	357.26	1.17	14.40
		$16 f_c^{0.5} h_{ef}^{1.6667}$	340.62	1.11	14.38
		$15.5 f_c^{0.5} h_{ef}^{1.6667}$	329.62	1.08	14.34

f_c – concrete cylinder compressive strength (N/mm²), h_{ef} – effective embedment depth (mm), d_h – diameter of anchor head (mm), N_u – mean breakout capacity in uncracked concrete according to formula (N), F – mean breakout capacity in uncracked concrete according to on-site test (N), E_c – elastic modulus of rock, G_f – rock fracture energy

Table 6. Braciszów mine, h_{ef} = 100 mm

Eq. No.	Remark	Formula	N_u [kN] according formula	Ratio N_u/F	Ratio $k_r = \frac{kF}{N_u}$
1	45 – degree cone model (37)	$N_u = 0.3 f_c^{0.5} \pi h_{ef}^2 \left(1 + \frac{d_h}{h_{ef}}\right)$	169.13	0.73	0.41
2	LEFM Eligehausen and Sawade (16)	$N_u = 2.1\left(E_c G_f\right)^{0.5} h_{ef}^{1.5}$	-	-	-
3	CCD method (10)	$N_u = 13.5 f_c^{0.5} h_{ef}^{1.5}$	168.21	0.73	18.62
	(12)	$15.5 f_c^{0.5} h_{ef}^{1.5}$	193.13	0.85	18.62
	(36)	$17 f_c^{0.5} h_{ef}^{1.5}$	211.85	0.91	18.62
4	CCD method (35,38) $h_{ef} \leq 280$ mm	$N_u = 6.585 f_c^{0.5} h_{ef}^{1.6667}$	177.07	0.76	8.63
		$N_u = 16.8 f_c^{0.5} h_{ef}^{1.6667}$	451.12	1.94	8.64
		$15.5 f_c^{0.5} h_{ef}^{1.6667}$	416.21	1.79	8.64

f_c – concrete cylinder compressive strength (N/mm^2), h_{ef} – effective embedment depth (mm), d_h – diameter of anchor head (mm), N_u – mean breakout capacity in uncracked concrete according to formula (N), F – mean breakout capacity in uncracked concrete according to on-site test (N), E_c – elastic modulus of rock, G_f – rock fracture energy

the direction perpendicular to the layering. As it is difficult to determine the orientation of the rock material layering in the natural rock mass, it seems reasonable to operate with the maximum force that lowers the rock structure. This ensures the safety of potentially designed machinery and equipment to execute the assumed technological process.

With the purpose of using the obtained research results in engineering practice, it seems more logical to propose a new formula describing the course of the breaking force of the anchor *F*, as a function of the embedment depth and rock permeability to compression, in the following form (7):

$$F\left(h_{ef},\, f_c\right) = 0{,}02 \cdot {f_c}^{0.73} \cdot {h_{ef}}^{1.33} \qquad (7)$$

Since a different character of the relationship between the pulling force as a function of the embedment depth and the compression strength of the studied rocks was found in the case of the "Braciszów" mine (Fig. 4), the proposed empirical model (8) is based on the data with the exception of the Braciszów mine results. Such a model explains the processes with higher consistency.

$$F\left(h_{ef},\, f_c\right) = 0.0006 \cdot {f_c}^{1.24} \cdot {h_{ef}}^{1.60} \qquad (8)$$

The graphical comparison of the considered relationships is shown in Figure 7. The approximation of test results by function (8) produces satisfactory results for most rock formations, which is vital for the potential planning of the sequential stripping technology with the use of undercut anchors.

In order to study the behaviour of the forces, separate investigations and complementary studies are required.

However, it can be noted that the calibration coefficients derived from the models as well as the power exponents for individual variables differ significantly from those proposed so far in the models for concrete. These findings confirm the results from the previously conducted analysis.

The evidence from this research shows that, in contrast to embedment in concrete, substantially greater variation in the range of pull-out force values should be expected in the tests conducted on anchors fixed in the rock mass. The scatter of results may be attributed to the sheer number of factors contributing to a greater uncertainty of results and inaccuracy of rock-anchor system strength forecasting. The grain composition of the rock is not as important as its stratification or cleavage. The results from the study extend the knowledge on the load-carrying capacity of anchors, which is the subject of numerous studies, e.g. Marcon et al. [1].

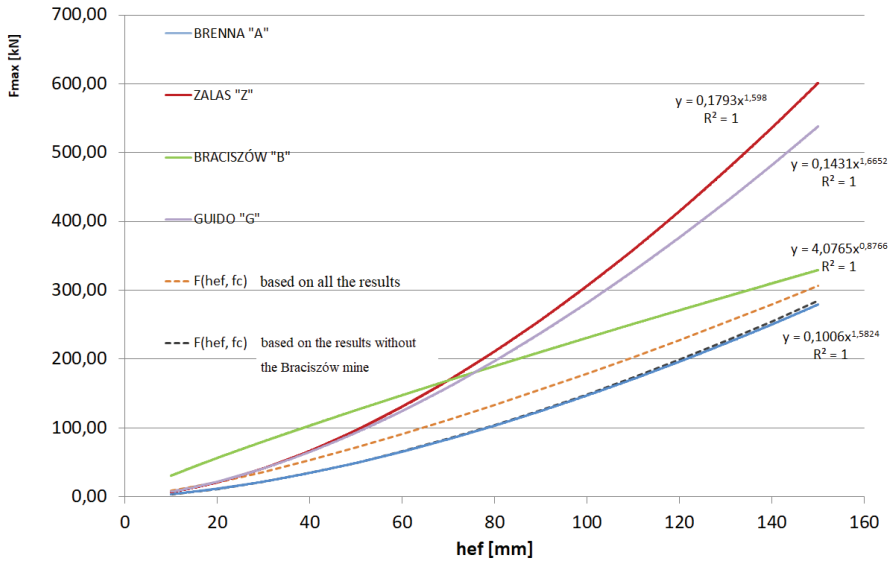

Fig. 7. The maximum breaking load (F_{max}) behaviour as a function of embedment depth (h_{ef}) and compression strength described by the new analytical model. The solid line – the model obtained from all test results, the broken line – the model after rejecting the measurement data from the Braciszów mine

CONCLUSIONS

The research was carried out on the rocks with a very large variety of strength parameters and internal structure. This resulted in a wider range of results obtained than in the case of concretes, which show the uniformity of structure and strength parameters on a macro scale.

In the case of rock materials, the load-bearing capacity of the anchor, as well as the values of the pull-out force, depend not only on the basic parameters of the rock, i.e. compressive strength and effective embedment depth, but also on the internal structure of the rock material.

The results from the experimental tests that were conducted under the conditions of stone mines and an underground coal mine (Guido) demonstrate the substantial discrepancy between the anchor pull-out force (anchor load-carrying capacity) for sandstone bed and the anchor pull-out force for concrete that was determined from empirical relationships.

Owing to the highly heterogeneous geological structure of sandstone bed in the test sites, the results are characterised by a large-degree inconsistency. Therefore, we postulate that, at the present stage, the relationships should be treated as estimates which require further research works. Nevertheless, bearing in mind the end goal of the research project, which is the estimation of the loading rates on the newly developed anchor design and, in particular, the drive mechanisms of the devices executing the rock fracture operation using the anchors in question, the results should be considered promising.

Furthermore, the anchorage solution presented here serves for the experimental purposes only. The system that is intended for use in industrial applications is currently undergoing the patenting process and, thus, cannot be presented in detail in this work. The concept employs undercut-burst anchors with a completely different operating principle and the drilling-anchoring device to enable full automation of the anchor embedment/breakout process.

The closest fit between the results from the field tests and predictions was obtained for the LEFM-based method. In part, this is due to a good estimation of the mechanical parameters of the sandstone from Brenna mine [2]. It was only in that case that it was possible to correctly calculate the stress intensity factor in fracture mode *I* (K_{Ic}) for estimating the fracture energy G_f.

For the present relationships of the pull-out force (9):

$$F_{CCD} = k_{nc} f_c^{0.5} h_{ef}^{1.5} \tag{9}$$

The values of the calibration factor k_{nc} were considerably higher in comparison with the current standardised data for concrete, that is from ~18 up to 31, depending on the sandstone strength.

For greater embedment depths [35]:

$$F_C = k_{nc} f_c^{0.5} h_{ef}^{1.666} \tag{10}$$

The value of the calibration factor from the relationship was in the range of ~8 to approx. 14,

which is, in fact, slightly below the currently followed standards.

In the light of the field tests and relevant calculations, the application of models and calculation procedures used in concrete theory to rock materials can lead to highly erroneous results.

New formulas of analytical models describe the development of the breaking force of the anchor fixtured in the rock material. The models incorporate significantly different values of calibration coefficients and power exponents than in the case of concrete. This allows for a much more precise estimation of the anchor breaking load in a natural brittle material, i.e. rock of a different internal structure. The proposed methodologies do not account for the rock quality parameters, such as the tension-compression asymmetry or the presence of fissures in the rock medium, which are widely employed in geomechanics. The impact of these factors was nonetheless reported in the study in the form of the considerable discrepancies in the measurement results in each of the individual mines (for the given rock formations and deposit conditions). The extension of the proposed empirical models and the appropriate calibration of these dependencies will enable more precise estimation of such parameters as the dimensions of the failure cone, the crack propagation or the value of the pull-out force.

Given the lack of knowledge in the field of anchor pull-out from the rock material, these findings should be treated as exploratory, but also as a valuable indication for further research.

The developed empirical models can also be useful for planning the typical anchor fixing processes in concrete fastening techniques. This significantly increases the existing state of the art in the field of anchoring techniques with the use of undercutting anchors.

Acknowledgements

This research project was financed in the framework of the Lublin University of Technology-Regional Excellence Initiative project, funded by the Polish Ministry of Science and Higher Education (contract no. 030/RID/2018/19).

REFERENCES

1. Marcon M, Ninčević K, Boumakis I, Czernuschka L-M, Wan-Wendner R. Aggregate Effect on the Concrete Cone Capacity of an Undercut Anchor under Quasi-Static Tensile Load. Materials 2018;11:711. https://doi.org/10.3390/ma11050711.
2. Gontarz J, Podgórski J, Jonak J, Kalita M, Siegmund M. Comparison Between Numerical Analysis and Actual Results for a Pull-Out Test 2019. https://doi.org/10.24423/EngTrans.1005.20190815.
3. Jonak J, Siegmund M. FEM 3D analysis of rock cone failure range during pull-out of undercut anchors. IOP Conference Series: Materials Science and Engineering 2019;710:012046. https://doi.org/10.1088/1757-899X/710/1/012046.
4. Jonak J, Siegmund M, Karpiński R, Wójcik A. Three-Dimensional Finite Element Analysis of the Undercut Anchor Group Effect in Rock Cone Failure. Materials 2020;13:1332. https://doi.org/10.3390/ma13061332.
5. Siegmund M, Jonak J. Analysis of the process of loosening the rocks with different strength properties using the undercutting bolts. IOP Conference Series: Materials Science and Engineering 2019;679:012014. https://doi.org/10.1088/1757-899X/679/1/012014.
6. Jonak J, Karpiński R, Siegmund M, Wójcik A, Jonak K. Analysis of the Rock Failure Cone Size Relative to the Group Effect from a Triangular Anchorage System. Materials 2020;13:4657. https://doi.org/10.3390/ma13204657.
7. Yang K-H, Ashour AF. Mechanism analysis for concrete breakout capacity of single anchors in tension 2008.
8. Anderson N.S: ICH Anchorage to Concrete Seminar. ACI 355.4-11, Qualification of Post-installed Adhesive Anchors in Concrete and Commentary. Seminar Santiago, Chile. 2015.
9. Shaikh AF and Yi, W. In-Place Strength of Welded Headed Studs. 318Reference 2011;D.
10. Eligehausen R, Mallée R, Silva JF. Anchorage in concrete construction. Berlin: Ernst & Sohn; 2006.
11. Fuchs W, Eligehausen R, Breen JE. Concrete Capacity Design (CCD) Approach for Fastening to Concrete. ACI STRUCTURAL JOURNAL 1995;92:73.
12. AEFAC STANDARD Part I. Design of post-installed and cast-in fastenings to concrete. Australian Engineered Fasteners and Anchors Council. AEFAC Standard – Part 1: public consultation draft 15/4/2015 n.d.
13. ETAG 001, Guideline for European technical approval of metal anchors for use in concrete. European Organisation for Technical Approvals, Brussels 1997.
14. Wyllie DC. Foundations on rock. 2nd ed. London ; New York: E & FN Spon; 1999.
15. Panton B. Numerical modelling of rock anchor pullout and the influence of discrete fracture net-

works on the capacity of foundation tiedown anchors 2016. https://doi.org/10.14288/1.0228651.

16. Brincker R, Ulfkjær JP, Adamsen P, Langvad L, Toft R. Analytical model for hook anchor pull-out n.d.:10.
17. Eligehausen R, Sawade G. A fracture mechanics based description of the pull-out behavior of headed studs embedded in concrete 1989. https://doi.org/10.18419/OPUS-7930.
18. Ljungberg J. Pullout test of rock bolts at the Lima Hydropower station- Assessment of th test method n.d.:58.
19. Asmus J, Eligehausen R. Design Method for Splitting Failure Mode of Fastenings. 2001.
20. Asmus J. Bemessung von zugbeanspruchten Befestigungen bei der Versagensart Spalten des Betons. Stuttgart: IWB; 1999.
21. Ballarini R, Yueyue X. Fracture Mechanics Model of Anchor Group Breakout. Journal of Engineering Mechanics 2017;143:04016125. https://doi.org/10.1061/(ASCE)EM.1943-7889.0001200.
22. Ballarini R, Keer LM, Shah SP. An analytical model for the pull-out of rigid anchors. International Journal of Fracture 33:75-94 1987:20.
23. Carpinteri A. Application of fracture mechanics to concrete structures. Journal of the Structural Division, Proceedings of the American Society of Civil Engineers, ASCE, VoI108, NoST4, 1982.
24. Karihaloo BL. Pull-out of axisymmetric headed anchors. Materials and Structures 1996;29:152–7. https://doi.org/10.1007/BF02486160.
25. Hirabayashi M, Suzuki T, Kobayashi K. Basic Study on Pullout Resistance Mechanism of Taper-tipped Post-installed Anchors. JR EAST Technical Review-No26 n.d.:6.
26. Momose M, Maruyama K, Shimizu K. Load carrying mechanism of anchor bolt. IABSE 1991. https://doi.org/10.5169/seals-47712.
27. Li L. Load bearing capacity of torque-controlled expansion anchors n.d.:8.
28. Zaidir, MARUYAMA K, SHIMOMURA T. Crack Growth Mechanism and Fatigue Strength of Concrete in Anchor System : Annual Papers on Concrete Engineering 1997;19:135–40.
29. Zhao G. Tragverhalten von randfernen kopfbolzenverankerungen bei betonbruch. Deutscher Ausschuss Fuer Stahlbeton 1995.
30. Vogel A, Ballarini R. Ultimate Load Capacities of Plane and Axisymmetric Headed Anchors. Journal of Engineering Mechanics 1999;125:1276–9. https://doi.org/10.1061/(ASCE)0733-9399(1999)125:11(1276).
31. Piccinin R, Ballarini R, Cattaneo S. Pullout Capacity of Headed Anchors in Prestressed Concrete. Journal of Engineering Mechanics 2012;138:877–87. https://doi.org/10.1061/(ASCE)EM.1943-7889.0000395.
32. Camposinhos RS. Undercut anchorage in dimension stone cladding. Proceedings of the Institution of Civil Engineers - Construction Materials 2013;166:158–74. https://doi.org/10.1680/coma.11.00050.
33. Barenblatt GI. The Mathematical Theory of Equilibrium Cracks in Brittle Fracture. Advances in Applied Mechanics, vol. 7, Elsevier; 1962, p. 55–129. https://doi.org/10.1016/S0065-2156(08)70121-2.
34. Nilforoush R, Nilsson M, Elfgren L, Ožbolt J, Hofmann J, Eligehausen R. Tensile Capacity of Anchor Bolts in Uncracked Concrete: Influence of Member Thickness and Anchor's Head Size. ACI Structural Journal 2017;114. https://doi.org/10.14359/51689503.
35. ACI Committee 318, American Concrete Institute (ACI). Building code requirements for structural concrete (ACI 318-14): an ACI standard and commentary on building code requerements for structural concrete (ACI 318R-14) : an ACI report. Farmington Hills, Michigan: American Concrete Institute, ACI; 2014.
36. ACI Committee 349. Code requirements for nuclear safety-related concrete structures: (ACI 349-06) and commentary, an ACI standard. Farmington Hills, Mich.: American Concrete Institute; 2006.
37. ACI Committee 349, "Design Guide to ACI 349-85", American Concrete Institute, Farmington Hills, MI, 1988.
38. ACI Committee 349, "Code Requirements for Nuclear Safety Related Structures (ACI 349-01)", American Concrete Institute, Farmington Hills, MI, 134 pp. 2001.
39. Pietruszczak S, Lydzba D, Shao JF. Modelling of inherent anisotropy in sedimentary rocks. International Journal of Solids and Structures 2002;39:637–48. https://doi.org/10.1016/S0020-7683(01)00110-X.
40. Podgórski J, Jonak J. Numerical tests of the influence of the orientation of stratification on the process of cutting of rocks. Mechanics and Control 2010;29.